Title
Regulation of cell reversal frequency in Myxococcus xanthus requires the balanced activity of CheY-like domains in FrzE and FrzZ

Journal
Molecular Microbiology, 100(2)

ISSN
0950-382X

Authors
Kaimer, Christine
Zusman, David R

Publication Date
2016-04-01

DOI
10.1111/mmi.13323

Peer reviewed

Regulation of cell reversal frequency in *Myxococcus xanthus* requires the balanced activity of CheY-like domains in FrzE and FrzZ

Christine Kaimer[1,2] and David R. Zusman[1,3]

[1]Department of Molecular and Cell Biology, University of California, Berkeley, CA 94720, USA

[2]Current address: Lehrstuhl für Biologie der Mikroorganismen, Ruhr-Universität Bochum, 44780 Bochum, Germany

[3]Corresponding author
Phone: (510) 642-2293
Fax: (510) 642-7038
E-mail: zusman@berkeley.edu

This article has been accepted for publication and undergone full peer review but has not been through the copyediting, typesetting, pagination and proofreading process which may lead to differences between this version and the Version of Record. Please cite this article as an 'Accepted Article', doi: 10.1111/mmi.13323

Summary

The Frz pathway of *Myxococcus xanthus* controls cell reversal frequency to support directional motility during swarming and fruiting body formation. Previously, we showed that phosphorylation of the response regulator FrzZ correlates with reversal frequencies, suggesting that this activity represents the output of the Frz pathway. Here, we tested the effect of different expression levels of FrzZ and its cognate kinase FrzE on *M. xanthus* motility. FrzZ overexpression caused a slight increase in phosphorylation and reversals. By contrast, FrzE overexpression abolished phosphorylation of FrzZ; this inhibition required the response regulator domain of FrzE. FrzZ phosphorylation was restored when both FrzE and FrzZ were overexpressed together. Our results show that the response regulator domain of FrzE is a negative regulator of FrzE kinase activity. This inhibition can be modulated by FrzZ, which acts as a positive regulator. Interestingly, fluorescence microscopy revealed that FrzZ and FrzE localize differently: FrzE co-localizes with the FrzCD receptor and the nucleoid, while FrzZ shows dispersed and polar localization. However, FrzZ binds tightly to the truncated variant FrzEΔ^{CheY}. This indicates that the response regulator domain of FrzE is required for the interaction between FrzE and FrzZ to be transient, providing an unexpected regulatory output to the Frz pathway.

Introduction

Myxococcus xanthus are soil-dwelling, Gram-negative bacteria with unique multicellular behaviors (Reichenbach, 1993, Zusman *et al.*, 2007). Vegetative cells are predatory on other microorganisms, although they can also grow on nutrients in their environment. They are usually found in large groups where they can effectively lyse prey bacteria or yeasts by secreting antibiotics or enzymes for the degradation of biomaterials. When resources become limiting, some cells aggregate to build fruiting bodies containing resistant spores while other cells either lyse or remain as resting cells (peripheral rods) that can rapidly resume growth should nutrients become available again.

The multicellular behavior of *M. xanthus* requires cell-to-cell communication as well as coordinated cell motility. For cell movement along surfaces, cells use two independent mechanisms (Hodgkin & Kaiser, 1979): the A-motility system utilizes laterally distributed gliding motors, whereas the S-motility system propels cells by the extension and retraction of polar Type IV pili (Li *et al.*, 2003, Nan & Zusman, 2011). A-motility is primarily used for the movement of isolated cells and is adapted for movement on firm surfaces, like 1.5% agar, while S-motility usually requires multicellular interactions and is adapted for softer surfaces, like 0.5% agar (Shi & Zusman, 1993). Neither motility system can function in liquid media, as the cells do not produce flagella.

As cells move on surfaces, individual cells periodically invert their polarity and reverse their direction of movement (Reichenbach, 1966, Kaimer *et al.*, 2012). At cell reversal, polar Type IV pili are disassembled at the old leading cell pole and reassembled at the lagging pole, which then becomes the new leading cell pole (Bulyha *et al.*, 2009). The cell polarity axis is established by three known regulatory proteins, MglA, MglB and RomR that are associated with the leading or lagging cell poles in an asymmetric pattern (Leonardy *et al.*, 2010, Zhang *et al.*, 2010, Keilberg *et al.*, 2012, Zhang *et al.*, 2012). It was recently observed that the MglA protein forms a concentration gradient from the leading cell pole towards the lagging cell pole, which biases the random reversals of a gliding motor protein to allow for the forward propulsion of the cell (Nan *et al.*, 2014). At cell

reversal, all three proteins MglA, MglB and RomR switch their position to the opposite cell poles, respectively, and cause the gliding motors to invert the direction of movement.

The frequency of cell reversals is important for coordinated movement. Under laboratory conditions, individual wild type cells move slowly at a velocity of 1-4 μm/min, and cells reverse their direction periodically on average every 8-10 min (Spormann & Kaiser, 1995). Strains with aberrant reversal frequencies are constrained in their spreading radius, and may be unable to form normal developmental aggregates and fruiting bodies (Bustamante *et al.*, 2004).

The Frz chemosensory system regulates cell reversal frequency, ensuring proper directional movements during vegetative growth as well as during development (Blackhart & Zusman, 1985, Zusman *et al.*, 2007). Previous studies have shown that signal transduction by the Frz pathway requires the receptor protein FrzCD, the histidine kinase FrzE and the coupling protein FrzA (Bustamante *et al.*, 2004). Furthermore, the activity of the FrzCD receptor is modulated by methylation, which is catalyzed by FrzF, a methyl transferase, and FrzG, a methyl esterase, and by an upstream regulator, FrzB (Scott *et al.*, 2008, Bustamante *et al.*, 2004, Astling *et al.*, 2006). The histidine kinase FrzE interacts with FrzCD and uses ATP as a phosphoryl-donor for autophosphorylation at a histidine residue. The phosphoryl-group is subsequently transferred to an aspartate residues of FrzZ, a dual CheY-like response regulator (Fig. 1). Phosphotransfer from FrzE to one or both of the CheY-like domains of the response regulator FrzZ has been demonstrated *in vitro* (Inclán *et al.*, 2007, Inclán *et al.*, 2008).

Mutations in Frz proteins can cause either hyper- or hypo-cell reversal frequencies. Cells that carry in-frame deletions of FrzCD, FrzA, FrzE or FrzZ cause hypo-cell reversals: cells reverse much less frequently than wild type, about once every 60 min. These strains show limited colony spreading on soft surfaces (e.g. 0.5% agar plates), and are unable to aggregate into fruiting bodies under starvation conditions; cells instead form unstructured, 'frizzy' filaments (Bustamante *et al.*, 2004, Blackhart & Zusman, 1985). By contrast, partial truncation of the N-terminus of the receptor FrzCD,

or a point mutation of the C-terminal response regulator domain of FrzE ($FrzE^{D709A}$) results in hyper-cell reversal frequencies (Bustamante *et al.*, 2004, Li *et al.*, 2005). Hyper-reversing cells show almost no net translocation: they form compact, non-spreading colonies on agar plates, and cannot form fruiting bodies or 'frizzy' filaments.

The periodic pole-to-pole switching of polarity proteins, and consequently the inversion of the motility motors, is dependent on Frz signaling, but it is not clear how signals from the Frz pathway are communicated to downstream regulators. Earlier reports based on the phenotypic analysis of double mutants suggested that the response regulator FrzZ acts as the most downstream component of the Frz pathway (Inclán *et al.*, 2007). Indeed, FrzZ localizes to the leading cell pole upon phosphorylation, making it a strong candidate to directly interact with proteins of the polarity system to modulate reversal frequency (Kaimer & Zusman, 2013). Here, we tested how cell reversals and motility behavior are affected by different expression levels of the response regulator, FrzZ and its cognate kinase, FrzE. Our experiments support the hypothesis that FrzZ is a positive modulator of FrzE activity, which indirectly controls cell reversals but which is not required for signal transfer under all conditions. The cellular localization of FrzZ and FrzE suggests a transient interaction of the two proteins that is regulated by the CheY-like domain of FrzE.

Results

FrzZ overexpression causes limited increases in FrzZ phosphorylation and cell reversal frequency

We recently observed that an increase in cellular reversal frequency in several *frz* mutants is positively correlated with the level of phosphorylated FrzZ in cell extracts (Kaimer & Zusman, 2013). This finding raised the possibility that the dual response regulator FrzZ acts in a concentration-dependent manner as a modulator of cellular reversal frequency. In order to test this hypothesis, we increased the expression level of FrzZ and its cognate kinase, FrzE, with the expectation that this would increase the level of phosphorylated FrzZ. Accordingly, we constructed strain DZ4850 (*ΔfrzZ* P_{Van}-*frzZ*), which expresses FrzZ from a vanillate-inducible promoter (Iniesta *et al.*, 2012) (Fig. 2A). The addition of increasing amounts of vanillate had no effect on motility behavior in wild type cells (Supplementary Figure SI 1). With strain DZ4850, FrzZ expression was dependent on vanillate concentration, as confirmed by Western blotting (Fig. 2B and C). In the absence of vanillate, FrzZ was expressed at background levels of about 0.16-fold relative to wild type, indicating very low expression but some leakage from the promoter. Under these conditions, the phenotype of strain DZ4850 was similar to a *ΔfrzZ* deletion mutant: cells displayed reduced swarming motility when spotted on 0.5% agar and were unable to form fruiting bodies upon starvation (Fig. 2D). Furthermore, individual cells reversed less frequently than wild type ($p < 0.01$), with a mean of 1.1±1.1 reversals in 30 min (mean±SD, n=80, Fig. 2E). However, addition of 10 μM vanillate induced FrzZ expression to wild type levels, and fully restored swarming motility on 0.5% agar as well as fruiting body formation upon starvation (Figs. 2C and D). The reversal frequency of individual cells reached an average of 2.3±1.5 reversals per 30 min, similar to the reversal frequency we observed for wild type under these conditions (2.1±1.1 reversals per 30 min) (Fig. 2E). When 500 μM vanillate was used to induce expression, FrzZ was overexpressed about 15-fold (Fig. 2C). Under these conditions, we observed normal fruiting body formation although swarming on 0.5% agar was

reduced (Fig. 2D). Cells displayed an average of 3.5±1.8 reversals in 30 min, significantly higher than in wild type (n= 80, $p < 0.01$) (Fig. 2E).

We then asked whether FrzZ phosphorylation increased upon FrzZ overexpression. For these experiments, cell extracts were separated by SDS-PAGE in the presence of Phos-tag, which allows the spatial separation of phosphorylated and non-phosphorylated proteins (Kaimer & Zusman, 2013, Kinoshita *et al.*, 2009) (Fig. 2F). FrzZ was subsequently analyzed by Western blotting with FrzZ-specific antisera. We were unable to detect phosphorylated FrzZ in the absence of vanillate. When 10 μM vanillate was added, we observed partial phosphorylation of FrzZ, similar to the amount observed in wild type cells. Interestingly, at 500 μM vanillate (15-fold overexpression of FrzZ), we observed an elevated level of phospho-FrzZ, although the fraction of phosphorylated to unphosphorylated FrzZ appeared similar to wild type cell extracts (Fig. 2F).

Overexpression of the His-kinase, FrzE, inhibits FrzZ phosphorylation

Since FrzZ, under all expression levels tested, showed only partial phosphorylation, we tried to increase the level of FrzZ phosphorylation by overexpressing its cognate His-kinase, FrzE. For these experiments, we constructed strain DZ4851 (*ΔfrzE* P_{lac}*frzE*), which expresses FrzE from an IPTG-inducible promoter (Iniesta *et al.*, 2012) (Fig. 3A). The expression of FrzE was quantified by Western blots using FrzE-specific antisera and a fluorescent secondary antibody. We found that in the absence of inducer, strain DZ4851 expressed two-fold elevated FrzE levels as compared to wild type, apparently due to a leaky IPTG-sensitive promoter (Fig. 3B and C). However, despite the two-fold overexpression, DZ4851 displayed motility behavior and fruiting body formation indistinguishable from wild type (Fig. 3D). Without the addition of inducer, individual cells of DZ4851 reversed on average 2.1±1.2 times per 30 min, identical to the frequency we observed for wild type cells in control experiments (Fig. 3E). Additionally, this strain showed phosphorylated FrzZ at a level similar to wild type, as determined by Phos-tag-SDS-PAGE (Fig. 3F). Thus, the

constitutive expression of FrzE from a non-native promoter allows normal behavior during vegetative growth and development. Addition of 10 μM or 50 μM IPTG to growth media resulted in 7-fold or 20-fold over-expression of FrzE, respectively (Fig. 3C). Surprisingly, FrzZ phosphorylation was not increased upon FrzE overexpression, but abolished completely, as determined by Phostag-SDS-PAGE (Fig. 3F). Upon addition of 10 μM IPTG, the frequency of cell reversals was significantly reduced to 0.8±0.9 per 30 min ($p < 0.01$), consistent with the loss of phosphorylated FrzZ; upon addition of 50 μM IPTG, we observed on average 0.6±0.7 reversals per 30 min (80 cells analyzed for each condition) (Fig. 3E). Cells displayed reduced motility and formed frizzy filaments, but no fruiting bodies on agar plates containing the respective concentrations of IPTG (Fig. 3D). By contrast, addition of increasing amounts of IPTG to wild type cells did not lead to abnormal behavior (Supplementary Figure SI 1). These observations suggest that Frz signaling is abolished upon overexpression of the FrzE His-kinase, indicating that FrzE has a concentration-dependent, negative regulatory effect on Frz signaling.

The inhibition of FrzZ phosphorylation by high FrzE levels is overcome by increasing FrzZ expression

Since overexpression of FrzE inhibited FrzZ phosphorylation, we wondered whether this inhibition could be countered by re-balancing the level of these proteins. We therefore constructed strain DZ4852 (Δ*frzZ* Δ*frzE* P_{Van}-*frzZ* P_{IPTG}-*frzE*) to independently control the expression of FrzZ and FrzE. In strain DZ4852, ectopic copies of *frzZ* and *frzE* genes are expressed under control of vanillate- and IPTG-inducible promoters, respectively, while the native genes of both *frzZ* and *frzE* were deleted. Thus, varying the amounts of the inducers vanillate or IPTG modulates the level of FrzZ and FrzE, respectively, in the same strain. However, we did not observe any effects on motility upon the combined addition of vanillate and IPTG to wild type cells (data not shown).

When both FrzE and FrzZ proteins were expressed at levels similar to wild type (10 μM vanillate and no IPTG added), strain DZ4852 resembled wild type with regards to motility behavior on 0.5% agar and starvation agar (Fig. 4A). We observed a mean of 2.9±0.9 cell reversals in 30 min, with 80 cells analyzed (Fig. 4B). Phostag-analysis showed FrzZ phosphorylation comparable to wild type levels (Fig. 4C). Overexpression of FrzZ, while FrzE was kept at wild type concentrations (500 μM Van, 0 μM IPTG, Fig. 4A), had similar effects as observed for strain DZ4850 described in Fig. 2. Overexpression of FrzE in the presence of wild type levels of FrzZ (10 μM Van and 10 μM IPTG), resulted in a similar, hypo-reversing phenotype as observed in strain DZ4851, confirming an inhibitory effect of FrzE (Fig. 4A).

Strain DZ4852 allowed us to test whether an increase in FrzZ could overcome the inhibitory effect. Overexpression of both FrzE and FrzZ (500 μM vanillate and 10 μM IPTG) caused cell motility to revert from hypo-reversing to wild type behavior. The mean number of cell reversals per 30 min in individual cells increased significantly ($p < 0.01$) from 1.4±0.1 (10 μM IPTG/10 μM Van) to 3.2±0.2 (10 μM IPTG/500 μM Van), with 80 cells analyzed for each condition (Fig. 4B). Motility behavior on 0.5% agar indicated a recovery from the hypo-reversing phenotype to wild type movements; also, these cells were able to form fruiting bodies on starvation media (Fig. 4A). Furthermore, FrzZ phosphorylation was restored when FrzZ was expressed at higher concentrations as well (10 μM IPTG, 500 μM Van) (Fig. 4C). Taken together, these experiments indicate that increasing the concentration of the response regulator FrzZ overcomes the concentration-dependent inhibitory effect of overexpressed FrzE. This implies that FrzZ acts as a positive modulator on FrzE activity.

The C-terminal response regulator domain of FrzE inhibits the phosphorylation of FrzZ

FrzE, in addition to the His-kinase domain (amino acids 270 to 509), contains a C-terminal response regulator (CheY) domain (amino acids 660 to 776) that can be phosphorylated at Asp709 (Fig. 1)

(Inclán *et al.*, 2008, Li *et al.*, 2005). *In vitro* experiments showed that phosphorylation of the response regulator domain directly interfered with autophosphorylation of the FrzE kinase domain (Inclán *et al.*, 2008). Deletion of the response regulator domain of FrzE resulted in increased FrzZ phosphorylation and about a two-fold increase in cell reversal frequency compared to wild type on 1.5% agar (Li *et al.*, 2005, Kaimer & Zusman, 2013). To test whether the inhibitory effect that we observed during FrzE overexpression depends on its C-terminal response regulator domain, we overexpressed FrzEΔ^{CheY} in a Δ*frzE* mutant background (strain DZ4853, Δ*frzE* P_{IPTG}-*frzE*Δ^{cheY}) (Fig. 5A). This strain showed similar expression levels of FrzEΔ^{CheY} in response to IPTG as we observed previously for full-length FrzE in DZ4852 (data not shown).

Cells expressing FrzEΔ^{CheY} displayed no swarming on 0.5% agar and formed fruiting bodies of slightly aberrant morphology, which is in agreement with earlier reports (Inclán *et al.*, 2008, Li *et al.*, 2005) (Fig. 5A). However, IPTG-induced overexpression of the kinase domain did not further change motility behavior, in contrast to strains overexpressing full-length FrzE. Colonies of strain DZ4853 grown on 0.5% agar or on starvation agar with 10 μM or 50 μM IPTG did not show significant differences compared to uninduced controls (Fig. 5A). Moreover, the average number of cell reversals, did not change at different levels of inducer. We observed 3.7/3.6/3.8 reversals per 30 min when 0/10/50 μM IPTG was added to control expression of FrzEΔ^{CheY} (Fig. 5B). In contrast to overexpression of full-length FrzE, overexpression of FrzEΔ^{CheY} did not abolish FrzZ phosphorylation. FrzZ in DZ4853 was phosphorylated at a higher level compared to wild type, presumably because the FrzE kinase is not inhibited by FrzE-CheY domain. At these increased phosphorylation levels, two signals can be detected for phosphorylated FrzZ, which represent phosphorylation at the two aspartate residues D52 and D220 (Kaimer & Zusman, 2013). Moreover, the level of FrzZ phosphorylation remained constant upon expression of FrzEΔ^{CheY} at varied concentrations (Fig. 5C). These experiments support the hypothesis that the concentration-dependent inhibition of FrzE activity is due to its C-terminal CheY-like response regulator domain. However,

detecting the phosphorylation of FrzZ provides only an indirect measure for FrzE kinase activity and FrzE may also phosphorylate other targets, e.g. FrzE-CheY.

Previous experiments showed that the inhibition of FrzE autophosphorylation by the response regulator domain of FrzE depends on the phosphorylation of Asp709, as the point mutation D709A results in reduced colony spreading and hyper-reversals (Fig. 5D) (Li *et al.*, 2005). When we expressed $FrzE^{D709A}$ at levels two-fold above wild type (no IPTG added) from the inducible P_{lac} promoter in strain DZ4854 (Δ*frzE* P_{IPTG}-$frzE^{D709A}$), cells displayed hyper-reversing phenotypes as expected, with 12.6±2.7 reversals per 30 min ($p < 0.01$ vs. wild type) (Fig. 5E). Furthermore, the level of phosphorylated FrzZ was elevated to 40% of FrzZ, compared to 3% phosphorylated FrzZ in wild type cells (Fig. 5F) (Kaimer & Zusman, 2013). Phosphorylated FrzZ was clearly detectable as two signals, representing phosphorylation at D52 and D220, respectively (Kaimer & Zusman, 2013). Overexpression of $FrzE^{D709A}$ upon addition of higher concentrations of IPTG did not markedly alter the motility behavior on hard and soft agar (Fig. 5D), nor change the phosphorylation level of FrzZ (Fig. 5F). These experiments indicate that the decrease in FrzE kinase activity observed when full-length FrzE is overexpressed is dependent on an active CheY-like response regulator domain phosphorylated at Asp709.

FrzZ is not required for wild type reversals in $FrzE^{D709A}$

FrzZ appears to be necessary for relieving the auto-inhibitory effect mediated by the C-terminal response regulator domain of FrzE, but it remains unclear whether FrzZ is indeed necessary to achieve cell reversals with frequencies typical for wild type. We therefore deleted FrzZ in strains that lack the auto-inhibitory effect provided by the response regulator domain in FrzE. We analyzed the phenotypes of strains DZ4868 (*ΔfrzZ ΔfrzE* P_{IPTG}-$frzEΔ^{cheY}$) and DZ4869 (*ΔfrzZ ΔfrzE* P_{IPTG}-$frzE^{D709A}$) in the absence of IPTG so that these proteins would have close to normal expression. Strain DZ4868 (*ΔfrzZ ΔfrzE* P_{IPTG}-$frzEΔ^{cheY}$) showed reduced swarm expansion on 0.5% agar and

frizzy filaments on starvation agar plates, consistent with a hypo-reversing phenotype and similar to the *ΔfrzZ ΔfrzE* double mutant (DZ4849) (Fig. 6A and data not shown). Indeed, the frequency of cell reversals was reduced to 1.4±1.1 reversals per 30 min compared to wild type ($p < 0.01$) (Fig. 6B). These results are in agreement with the previously reported phenotype of a similar mutant strain, DZ4703 (*ΔfrzZ frzEΔ*^{cheY}) (Inclán *et al.*, 2007). By contrast, strain DZ4869 (*ΔfrzZ ΔfrzE* P_{IPTG}-*frzE*^{D709A}), which combines a deletion of FrzZ with the mutated variant FrzE^{D709A}, reproducibly showed wild type behavior with respect to motility on 0.5% agar and fruiting body formation (Fig. 6A). On average we detected 3.4±1.5 reversals per 30 min in individual cells (80 cells analyzed) (Fig. 6B). These experiments show that Frz signaling requires the presence of the FrzE response regulator domain, but not its phosphorylation. If the response regulator domain of FrzE is incapable of being phosphorylated, but is still present as in FrzE^{D709A}, FrzZ may not be required for reversal control. These results suggest that the response regulator domain of FrzE has an additional function, perhaps by interacting with an unidentified protein, and that FrzZ is then required to modulate FrzE.

FrzE co-localizes with FrzCD and the bacterial nucleoid

Previously, we showed that FrzZ is a cytoplasmic protein that is recruited to the leading cell pole upon phosphorylation, but re-localizes to the opposite cell pole during cell reversals (Kaimer & Zusman, 2013). We were therefore interested in determining the localization of FrzE since FrzZ and FrzE must interact during Frz signaling. To visualize FrzE by fluorescence microscopy, we first constructed a strain (DZ4855, *ΔfrzE* P_{Van}*-frzE-yfp*) that expresses yellow fluorescent protein (YFP)-labeled FrzE from a vanillate-inducible promoter. The level of FrzE-YFP was comparable to wild-type FrzE without the addition of vanillate due to a leaky promoter (data not shown). FrzE-YFP was able to complement FrzE with respect to the regulation of motility behavior and fruiting body formation indicating that labeled FrzE-YFP is functional (Fig. 7A). Fluorescence microscopy revealed that FrzE-YFP is primarily localized at non-polar regions of the cytoplasm in several irregular clusters, which in most cases cover about half of the cell length (Fig. 7B, left panel). In many cells, FrzE-YFP was clearly visible in several separated foci (Fig. 7B, right panels). The clusters formed by FrzE remained within the mid-cell area during cell movement and cell reversals (data not shown).

Since FrzE and the FrzCD were previously shown to interact *in vitro* (Inclán *et al.*, 2007) and the localization pattern of FrzE-YFP appeared similar to the localization of the cytoplasmic FrzCD chemoreceptor (Mauriello *et al.*, 2009), we wondered whether these proteins co-localize. To test the localization of FrzE and FrzCD simultaneously, we constructed strain DZ4858 (P_{Van}*-frzE-yfp frzCD-mCherry*) that expresses FrzE-YFP and FrzCD-mCherry (replacing the original FrzCD) in the same cell. Both FrzCD-mCherry and FrzE-YFP formed cellular clusters that also were observed with the labeled proteins individually (Fig. 8A). Analysis of mCherry and YFP fluorescence profiles in the same cell shows that FrzCD and FrzE indeed fully co-localize within the cell (Fig. 8B), supporting the interaction of both proteins in cellular clusters. We noted, however, that strain DZ4858 did not

show wild type motility behavior, but reduced cell reversals (data not shown). Presumably, the dual labeling of the two Frz proteins interferes with their function.

The clusters formed by FrzE and FrzCD did not fill the entire cell, but occupied about half of the cell area towards mid-cell; they were never localized at the cell poles (Fig. 8A). This pattern is reminiscent of the distribution of the bacterial nucleoid, which prompted us to include DNA stain (Hoechst 33342 at 1 µg/ml) in our experiments. Strikingly, the localization of FrzE and FrzCD clusters overlapped with the localization of the nucleoid; clusters were never observed in an area of the cell that was devoid of DNA (Fig. 8A). These observations were supported by analysis of the intensity profile of fluorescence signals in several cells. Signals of YFP, mCherry and Hoechst stain channels showed clear overlap of high intensity regions, indicating co-localization of FrzE and FrzCD with the nucleoid (Fig. 8B).

FrzE localization depends on FrzCD and FrzA, but not on FrzZ

To further investigate the determinants of FrzE localization, we visualized FrzE-YFP in different Frz pathway mutants, by transforming deletion mutants Δ*frzCD*, Δ*frzA* or Δ*frzZ*, respectively, with plasmid encoded P_{Van}-*frzE-yfp*. All three strains displayed hypo-reversing motility phenotypes, as expected for their respective mutations in the Frz pathway (data not shown). In the absence of FrzCD (DZ4859, Δ*frzCD* P_{Van}-*frzE-yfp*), FrzE-YFP did not form defined clusters but showed dispersed localization, indicating that FrzCD directly or indirectly determines the localization of FrzE in the nucleoid region. However, deletion of FrzCD did not lead to a uniform distribution of FrzE-YFP. (Fig. 8C). The addition of DNA stain to samples revealed that in the absence of FrzCD, FrzE accumulated in areas devoid of DNA (Fig. 8C and D). Localization of FrzE-YFP to the nucleoid region was also lost upon deletion of the coupling protein FrzA (DZ4860, Δ*frzA* P_{Van}-*frzE-yfp*), which presumably serves as an adapter for the interaction of FrzE with FrzCD (Bustamante *et al.*, 2004, Inclán *et al.*, 2007). Lack of FrzA resulted in a diffuse FrzE-YFP distribution, and exclusion

from the nucleoid area (Fig. 8C and D). By contrast, in the absence of the FrzZ response regulator (DZ4861, Δ*frzZ* P_{Van}-*frzE-yfp*), FrzE-YFP formed cellular clusters associated with the nucleoid, indistinguishable from wild type (Fig. 8C and D). These observations suggest that FrzE does not have intrinsic affinity for the nucleoid, but that cluster formation and nucleoid association depend on the FrzCD chemoreceptor and are mediated by the coupling protein FrzA. Furthermore, the response regulator FrzZ is not required for correct FrzE localization, or for its interaction with FrzCD.

The response regulator domain of FrzE determines FrzZ localization

We previously showed that phosphorylated FrzZ predominantly localizes to the leading cell pole, while unphosphorylated FrzZ is distributed throughout the cytoplasm (Kaimer & Zusman, 2013) (Fig. 9A). To determine the cellular localization of both FrzZ and FrzE in the same cells, we constructed strain DZ4865 (Δ*frzE* P_{Van}-*frzE-mCherry frzZ-gfp*) that combines FrzE-mCherry expression at low levels (P_{Van} without the addition of inducer), with FrzZ-GFP expression from its native promoter. Even though the fluorescent fusions of FrzZ and FrzE are fully functional when expressed individually, strain DZ4865 showed the hypo-reversing Frz phenotype. However, fluorescence microscopy showed the expected localization patterns for FrzE and FrzZ: FrzZ-GFP accumulated in a faint cluster at the leading cell pole (green triangle), and appeared diffusely distributed in the cytoplasm (Fig. 9B); by contrast, FrzE-mCherry formed several cellular clusters (red triangles), but did not localize at either cell pole. The fact that we did not see these proteins co-localize suggests that the interaction between full-length FrzE and FrzZ is transient and is not easily captured by fluorescence microscopy in live cells.

FrzZ-GFP changed its localization pattern in a *frzEΔ*^{cheY} background, in which the C-terminal CheY-like domain of FrzE was removed (DZ4857, *frzEΔ*^{cheY} *frzZ-gfp*). In this case, in addition to the focus at the leading cell pole, FrzZ formed one or two distinct cellular clusters (Fig. 9C). We constructed strain DZ4866 (*frzZ-gfp ΔfrzE* P_{Van}-*frzEΔ*^{cheY}*-mCherry*) to compare the localization of

FrzZ-GFP and FrzEΔ^{CheY}-mCherry. The C-terminally truncated variant FrzEΔ^{CheY}-mCherry formed one to two distinct cellular clusters (red triangles), similar to FrzZ-GFP (Fig. 9D). Fluorescence of FrzZ-GFP clearly overlapped with FrzEΔ^{CheY}-mCherry in cellular clusters (yellow triangles). However, we never detected FrzEΔ^{CheY}-mCherry at the cell poles, but only observed polar FrzZ-GFP foci (green triangles) (Fig. 9D).

When cells expressed FrzE^{D709A} in strain DZ4864 (*frzZ-gfp* Δ*frzE* P_{IPTG}-*frzE*^{D709A}) we observed FrzZ-GFP at the leading cell pole only (Fig. 9E). These cells hyper-reverse, and FrzZ-GFP switches to the opposite cell pole at each reversal (data not shown). FrzE^{D709A}-YFP itself shows a localization pattern similar to that of FrzE-YFP, with several clusters formed in the mid-cell area (Fig. 9F, strain DZ4870, Δ*frzE* P_{Van}-*frzE*^{D709A}-*yfp*).

Our data suggest that the interactions of the FrzE His-kinase with the FrzZ response regulator are disturbed by phosphorylation of FrzE^{CheY}. In wild type cells, or when FrzE^{CheY} is not phosphorylated in FrzE^{D709A}, FrzZ dissociates from FrzE after phosphorylation and is recruited to the leading cell pole. In the absence of FrzE^{CheY}, a significant portion of FrzZ remains bound to FrzE. Possibly, the response regulator domains in FrzE and FrzZ compete for binding and phosphotransfer from the FrzE kinase domain.

Discussion

The Frz chemosensory pathway controls the frequency of cell reversals to support coordinated multicellular behavior in *M. xanthus* (Blackhart & Zusman, 1985). Signal transmission involves protein homologues typically found in bacterial chemotaxis pathways (Fig. 10A): FrzCD is a cytoplasmic receptor, FrzA is a CheW-like coupling protein, FrzE is a CheA-like His-kinase with a C-terminal CheY-like response regulator domain, and FrzZ is a dual response regulator protein with two CheY-like domains (Fig. 1) (Bustamante *et al.*, 2004). In this study, we investigated the role of the dual response regulator FrzZ and its interplay with its cognate His-kinase, FrzE, to address the molecular mechanism of Frz signaling.

We previously found that the frequency of cell reversals increases with the phosphorylation level of FrzZ. Moreover, FrzZ is recruited to the leading cell pole upon phosphorylation, which suggested a central role for FrzZ in transferring the Frz signal to downstream regulators that are located at the cell poles (Kaimer & Zusman, 2013). However, a Δ*frzZ* deletion mutant is still able to respond to repellents, unlike a Δ*frzE* or Δ*frzCD* mutant, suggesting that FrzZ is not required for signal transmission under all conditions (Bustamante *et al.*, 2004). We therefore began a series of experiments to clarify the role of FrzZ in regulating cell reversals.

Prompted by earlier observations, we addressed the possibility that the regulatory function of FrzZ is concentration-dependent, and tested the effect of FrzZ and FrzE overexpression. We observed that FrzZ overexpression reduced swarming motility on 0.5% agar, where cells utilize S-motility, while fruiting body formation on 1.5% agar was not compromised. Next, we overexpressed FrzE, the His-kinase, in an attempt to increase the cellular level of phosphorylated FrzZ. Unexpectedly, we found that FrzZ phosphorylation was inhibited when full length FrzE was overexpressed, reducing cell reversals, cell motility and fruiting body formation. However, FrzZ phosphorylation was restored when expression of both FrzZ and FrzE were increased concomitantly. Cells that expressed both, FrzE and FrzZ, at high levels showed normal cell reversal frequencies,

motility, and fruiting body formation. This indicates that the concentration-dependent auto-inhibitory effect of FrzE can be overcome by increasing FrzZ expression. The inhibitory effect of FrzE overexpression is mediated by the response regulator domain of FrzE, since the C-terminally truncated variant FrzEΔ^{CheY} showed activity at all expression levels. This is in agreement with previous *in vitro* experiments that showed that the C-terminal CheY-like domain of FrzE inhibits FrzE autophosphorylation (Inclán *et al.*, 2008, Li *et al.*, 2005). Our data suggest that FrzZ directly counters the inhibitory effect of FrzE^{CheY} (Fig. 10B).

FrzE^{CheY} accepts a phosphoryl-group from the FrzE kinase domain at a conserved aspartate residue, Asp709 (Inclán *et al.*, 2008). Mutation of this site in FrzE^{D709A} results in hyper-reversals, and cells are impaired in colony expansion and fruiting body formation (Li *et al.*, 2005). We found that in *M. xanthus* carrying FrzE^{D709A}, FrzZ is phosphorylated at high levels independently of the expression level. This indicates that phosphorylation of the CheY-like domain at Asp709 is required for the autoinhibitory effect of FrzE, consistent with *in vitro* experiments.

Interestingly, we found that cells show wild type behavior if *frzZ* is deleted in *frzE^{D709A}* expressing cells. This shows that in the absence of FrzE^{D709} phosphorylation, FrzZ function is not essential for the transmission of the Frz signal to downstream regulators. By contrast, deletion of *frzZ* in cells that carry wild type FrzE or a deletion in the entire response regulator domain of FrzE (FrzEΔ^{CheY}) results in the frizzy, hypo-reversing phenotypes (Fig. 6 and (Inclán *et al.*, 2007)). Apparently the presence, but not the phosphorylation, of a CheY-like domain of FrzE is required for normal Frz signaling. We noted that cells did not show hyper-reversing phenotypes without FrzZ, despite the enhanced phosphorylation capacity of the FrzE^{D709A} point mutant. This indicates that FrzZ is required to convey cell reversals at high frequencies, which is in agreement with the previous observation that FrzZ is required to mediate hyper-reversals in the *frzCD^{c}* (constitutively 'on') mutant (Inclán *et al.*, 2007, Guzzo *et al.*, 2015).

Since the regulation of motility and cell polarity in *M. xanthus* are coupled to the spatial distribution of protein regulators we determined the localization pattern of FrzE. FrzE co-localized with FrzCD in multiple cytoplasmic clusters and, surprisingly, these clusters also co-localized with the bacterial nucleoid. FrzE localization was dispersed in both a *ΔfrzCD* and a *ΔfrzA* mutant, indicating that FrzE cluster formation depends on its interaction with FrzCD and the coupling protein FrzA.

Our co-localization studies of full length FrzE and FrzZ showed that the localization of these proteins rarely overlap, even though FrzE phosphorylates FrzZ. FrzZ was dispersed throughout the cell, while the minor phosphorylated portion was sequestered at the leading cell pole; FrzE, on the other hand, was localized in distinct non-polar clusters. This suggests a transient interaction between FrzE and FrzZ that was not captured by fluorescence microscopy. However, the association of FrzE and FrzZ changed in cells lacking the response regulator domain of FrzE: the fluorescence signals for FrzZ and FrzEΔ^{CheY} clearly overlapped in distinct cellular clusters, but never at the cell pole. By contrast, FrzZ accumulated at the cell pole in a *frzE^{D709A}* mutant, while FrzE^{D709A} formed cellular clusters similar to FrzE. This suggests that FrzZ binds more strongly to FrzEΔ^{CheY} than to wild type FrzE or FrzE^{D709A}. Possibly, the CheY-like domains of FrzZ and FrzE^{CheY} compete for binding of the FrzE CheA-like kinase domain.

The close association of the CheA-like His-kinase FrzE with its chemoreceptor FrzCD are commonly observed in many bacterial chemosensory systems, although in most cases the receptor/kinase clusters are anchored to the cell membrane, and are often located at the cell poles (Mauriello, 2013, Jones & Armitage, 2015). In case of the Frz chemosensory clusters the association of with the nucleoid may ensure that the complexes are equally distributed among the daughter cells, since DNA is reliably segregated at cell division. Furthermore, the sequestering of phospho-FrzZ to the leading cell pole could play an additional role in modulating FrzE kinase activity, as the cell poles typically lack DNA in *M. xanthus*, and consequently also lack the FrzCD/FrzA/FrzE clusters.

Taken together, our experiments suggest that the three CheY-like response regulator domains of the Frz pathway constitute a regulatory unit to control the activity of the FrzE His-Kinase (Fig. 10B). The $FrzE^{CheY}$ domain acts as an inhibitor of the FrzE His-kinase domain and reduces cell reversal frequency, while the $FrzZ^{CheY}$ domains stimulate FrzE kinase activity. In wild type cells, the balanced action of the $FrzZ^{CheY}$ and $FrzE^{CheY}$ domains sets the interval between reversals to 8-10 min. Since FrzZ acts as a positive modulator on full length FrzE, we assume that this interaction directly counters the inhibitory effect of $FrzE^{CheY}$. Possibly, the $FrzZ^{CheY}$ domains compete with the $FrzE^{CheY}$ domain for phosphoryl-groups donated by the CheA-like FrzE kinase domain. This hypothesis is supported by the observation that FrzZ is tightly associated with the FrzE kinase domain ($FrzE\Delta^{CheY)}$, as shown by fluorescence microscopy (Fig. 9), and that FrzZ is phosphorylated at higher levels if the $FrzE^{CheY}$ domain is unable to accept phosphoryl-groups from the FrzE kinase, as in $FrzE^{D709A}$.

FrzE, which has both an activating and inhibiting effect, is central to Frz signaling. In contrast, we found that FrzZ is expendable to setting wild type reversal frequency in the *frzE*^{D709A} mutant. Interestingly, Guzzo *et al.* recently established a novel assay to analyze single cell reversals under S-motility conditions, and found that FrzZ is not required for reversals by the S-motility system (Guzzo *et al.*, 2015). It is therefore possible that FrzE directly targets an additional protein for phosphorylation, which is necessary to induce cell reversals. The response regulator RomR has been discussed as a substrate for FrzE. RomR directly or indirectly recruits MglA to the cell pole, and is therefore essential to establish cell polarity (Zhang *et al.*, 2012, Keilberg *et al.*, 2012). While genetic evidence was presented that RomR acts downstream of Frz signaling (Leonardy *et al.*, 2010), the Frz-dependent phosphorylation of RomR remains to be verified experimentally.

FrzZ plays an important role in the regulation of cell reversal frequency because increasing amounts of phospho-FrzZ leads to an increase in cell reversals. In two-component systems of other species, accessory CheY-like regulators were described to act as phosphate sinks, i.e. they solely

accept phosphoryl-groups from a His-kinase in order to modulate the phosphorylation rate of the main CheY-effector of the system (Sourjik & Schmitt, 1998, Amin *et al.*, 2014). Does a similar mechanism apply for Frz signaling? FrzZ and FrzE^{CheY} are both phosphorylated by the FrzE kinase, and presumably compete for phosphoryl-groups. However, neither phosphorylation of FrzE^{CheY} nor of FrzZ^{CheY} are required for wild type cell reversals, indicating that none of these CheY-like domains function as the principal effector in signal transmission to downstream regulators. Moreover, phosphorylated FrzZ is required to convey hyper-reversals, a function that is independent of FrzE^{CheY} but appears to depend on FrzZ recruitment to the leading cell pole (Kaimer & Zusman, 2013). We therefore speculate that FrzZ and FrzE^{CheY} do not act as a phosphate sink for each other. However, it is possible that the three CheY-like domains of FrzZ and of FrzE^{CheY}, in combination, constitute a phosphate sink to positively and negatively regulate the phosphorylation of an unknown effector. This would add a new level of complexity to bacterial two-component systems, which, in case of *M. xanthus*, might be necessitated by the coordination of two independent motility systems. Indeed, an analysis of the phylogenetic relationships of motility systems and their regulators revealed that the acquisition of FrzZ may coincide with the emergence of A-motility in addition to S-motility (Guzzo *et al.*, 2015).

Another scenario for the positive modulation of His-kinase activity was described for the two-component network that governs cell cycle progression in *Caulobacter crescentus* (Paul *et al.*, 2008). There, a single domain response regulator, DivK, binds to the catalytic core of its cognate kinases PleC and DivJ, and enhances their autophosphorylation activity. Moreover, DivK is a diffusible factor that interconnects spatially separate components of the regulatory system, which are located at opposite cell poles. In *M. xanthus*, FrzZ is a diffusible modulator that might connect the positive regulation of its cognate kinase, which is sequestered by the nucleoid, to downstream effectors at the cell pole.

Experimental procedures

Bacterial strains and growth conditions

M. xanthus strains were grown in CYE medium (10 mM MOPS, pH 7.6, 1% Casitone, 0.5% yeast extract and 4 mM $MgSO_4$; (Campos *et al.*, 1978)) at 32°C and 200 rpm. 1.5% agar was added for the preparation of agar plates. Antibiotics were used in the following concentrations: ampicillin 100 µg ml^{-1}, kanamycin 100 µg ml^{-1}, tetracycline 12.5 µg ml^{-1}. When appropriate, vanillate and IPTG were added to growth media as indicated in the text. *E. coli* strain DH5α was used for plasmid construction, and cultured in Luria-Bertani medium at 37°C.

Strain construction

M. xanthus strains used in this study are listed in Table 1. A comprehensive list of oligonucleotides and plasmids can be found as Supporting Information, Table SI 1 and Table SI 2, respectively.

A double deletion of *frzZ* and *frzE* coding sequences was obtained by transformation of DZ4484 with plasmid pJPM3. Kanamycin-resistant transformants were grown in CYE medium without antibiotics and selected for growth on 2.5% galactose, and loss of kanamycin resistance. Deletion of *frzZ* and *frzE* was confirmed by PCR and Western blot analysis. Strain DZ4849 was used to combine inducible variants of FrzE in pMR3487 and FrzZ in pMR3690 (see below). Transformants were subsequently selected for tetracycline and kanamycin resistance.

For the controlled overexpression of Frz proteins we used a series of plasmids generated by Iniesta *et al.* (2012). pMR3487 (tet^R) allows controlled expression from an IPTG-inducible promoter and integrates into the *M. xanthus* chromosome at a 1.38 kb-platform via single homologous recombination. pMR3690 (kan^R) is used for expression from a vanillate-inducible promoter and integrates at the MXAN_0018/0019-site. pMR3561 (kan^R) and pMR3562 (tet^R) integrate into the 1.38kb-platform and allow the expression of C-terminal fusions to YFP from a vanillate-inducible promoter (Iniesta *et al.*, 2012).

For IPTG-inducible expression of FrzE and FrzE variants, the coding sequence was amplified from DNA from *M. xanthus* wild type or mutant strains using primers C325 and C326, and cloned to *Kpn*I and *Xba*I sites of pMR3487. The resulting plasmid was used to transform DZ4481 or DZ4849, and transformants were selected for tetracycline resistance.

For vanillate-inducible expression of FrzZ variants, the coding sequences were amplified with primers C285 and C302, and cloned to the *Eco*RI and *Nde*I sites of pMR3690. Transformants in DZ4484 were selected for kanamycin resistance.

To construct fluorescent fusions of FrzE, the coding sequence of FrzE or of FrzE mutant variants was amplified from chromosomal DNA of *M. xanthus* wild type or the respective mutant strains with primers C282 and C283, and cloned to *Nde*I and *Eco*RI sites of pMR3562. For fusions to mCherry, amplified mCherry coding sequence (primers C269 and C270) was cloned to the *Eco*RI and *Nhe*I sites of pMR3562 to replace EYFP in pCK244. Plasmids 3562-*frzE-yfp* or 3562-*frzE-mCherry* were used to transform various *M. xanthus* mutant strains as indicated in the strain list. Transformants were selected for tetracycline resistance.

Determination of motility and developmental phenotypes

M. xanthus strains were cultured to exponential phase in liquid CYE medium, harvested by centrifugation at 8000 *g* for 10 min, washed once with MMC buffer (10 mM MOPS pH 7.6, 4 mM $MgSO_4$, 2 mM $CaCl_2$) and diluted to 4 x 10^9 cells ml^{-1} in MMC buffer. 5 µl of the suspension was spotted on CYE plates containing 0.5% agar to monitor motility behavior. To determine fruiting body formation upon starvation, 5 µl cell suspension was spotted on CF agar plates (10 mM MOPS pH 7.6, 8 mM $MgSO_4$, 1 mM KH_2PO_4, 0.015% Casitone, 0.2% sodium citrate, 0.1% sodium pyruvate, 0.02% $(NH_4)_2SO_4$, 1.5% agar; (Hagen *et al.*, 1978). Agar plates were incubated at 32°C in the dark and phenotypes were documented using a Nikon SMZ500 stereo microscope after 48 h (motility behavior on 0.5% agar), or after 96 h (fruiting body formation on starvation agar).

Preparation of cell extract for SDS-PAGE

M. xanthus cells were grown on CYE agar plates containing vanillate and/or IPTG as indicated. After 2 days of growth at 32˚C, cells were scraped off the plate and resuspended in ice cold PBS buffer with 1% Triton X-100. Suspensions were sonicated briefly and cell debris was removed by centrifugation for 2 min at 13000 rpm, 4˚C. The protein content of cell extracts was determined by the Bradford method and concentrations were normalized to 5-10 µg/ml. Cell extracts were mixed with 2x SDS-sample buffer, boiled for 5 min and separated on a 10 or 12% SDS-polyacrylamide gel, followed by Western blotting to nitrocellulose membrane and detection with specific antisera. Primary anti-FrzZ and anti-FrzE antibodies were used in 1:5000 or 1:1000 dilution, respectively. Secondary anti-rabbit or anti-mouse HRP-fused antibodies were diluted 1:5000. For quantification of Western blot bands, fluorescent IRDye secondary antibody was used in 1:3000 dilution, membranes were scanned with a infrared fluorescence scanner (Odyssey, Li-Cor) and signal intensity was analyzed using ImageStudio software.

Phos-tag experiments

The phosphorylation of FrzZ protein by Phos-tag SDS-PAGE was determined as described earlier (Kaimer & Zusman, 2013). Briefly, cell extracts of *M. xanthus* strains were separated by SDS-PAGE in gels containing 7.5% polyacrylamide and 50 µM Phos-tag compound (Wäko Chemicals) and 100 µM $MnCl_2$. After electrophoresis, gels were washed with EDTA-containing blotting buffer and proteins were transferred to nitrocellulose membrane by Western blot. Membranes were probed with primary anti-FrzZ specific antiserum and secondary anti-rabbit HRP-fused or fluorescent antibody.

Microscopy

Exponentially growing *M. xanthus* cells were diluted to 4 x 10^8 cells ml^{-1}, and 5 µl of the suspension were spotted on thin agarose pads (1.5% agarose in CF salts) on slides, and covered with a cover glass. Vanillate and IPTG were added to agarose pads as indicated in figure legends. Slides were incubated for 30-60 min at 32°C in the dark prior to image acquisition. For fluorescence microscopy, image acquisition was performed on a DV Elite microscope setup (Applied Precision) equipped with a CCD camera (CoolSnap HQ, Photometrics) and solid state illumination using filters of 461/489 nm for GFP and YFP, 529/556 nm for mCherry and 381/399 nm for Hoechst stain. All statements regarding the localization of fluorescent protein fusions are based on three or more independent microscopy experiments in which > 200 viable cells were observed.

Determination of cell reversal frequency

M. xanthus strains were grown to exponential phase in CYE medium containing vanillate or IPTG as indicated. Cells were diluted to 4 x 10^8 cells ml^{-1}, spotted to thin pads of CYE agar on object slides and covered with a cover glass. Agar pads contained inducers when applicable. Object slides were incubated in the dark for 1-3 h prior to imaging. Time-lapse sequences were obtained for 30 min at 20 sec intervals. Cell reversals of individual cells were counted manually. For each strain, at total of 80 individual cells from at least three independent experiments was analyzed. Statistic significance was determined by pairwise comparison of the different populations using the Mann-Whitney-Wilcoxon test (Supplementary Table SI 3).

Acknowledgements

We thank Montserrat Elias-Arnanz (Universidad de Murcia) for the kind gift of pMR-vectors, Emilia Mauriello (CNRS Marseille) for the construction of the FrzCD-mCherry fusion and Beiyan Nan (Texas A&M University) for discussion. This work was supported by a fellowship from the

Deutsche Forschungsgemeinschaft (DFG Ka 3361/1-1 and Ka 3361/2-1 to C.K.), and a grant from the National Institutes of Health (GM 020509 to D.R.Z.).

Figure Legends

Figure 1: Domain organisation of the FrzE His-kinase and the FrzZ response regulator. FrzE and FrzZ are part of the Frz signaling pathway, which controls cell reversal frequency in *M. xanthus*. FrzE autophosphorylates at a histidine residue (H49) of the N-terminal histidine phosphotransfer (Hpt) domain. The phosphoryl-group is subsequently transferred to an aspartate (D709) in the CheY-like response regulator domain at the C-terminus of FrzE, or to the two CheY-like domains (D52 and D220) of the response regulator FrzZ. Numbers indicate amino acid positions.

Figure 2: Overexpression of FrzZ affects cell motility and reversal frequency. (A) A copy of *frzZ* under the control of a vanillate-inducible promoter (P_{Van}) was introduced to a Δ*frzZ* background (strain DZ4850, Δ*frzZ* P_{Van}-*frzZ*). **(B)** Vanillate-dependent increase of FrzZ concentration in strain DZ4850 in the presence of 0, 10 or 500 µM vanillate (Van). FrzZ protein was detected in cell extracts by Western blot with FrzZ-specific antiserum. **(C)** Signal intensity for FrzZ protein as shown in (B) was quantified, and normalized to wild type (mean±SD). Data represent three independent experiments. **(D)** FrzZ overexpression slightly reduces motility on 0.5% agar. Strain DZ4850 was spotted to soft CYE plates (0.5% agar) or to starvation agar containing vanillate, as indicated. Motility and fruiting body formation were documented after 48 h or 96 h of incubation at 32°C, respectively. **(E)** Individual cells overexpressing FrzZ show a moderate increase in cell reversal frequency. Cells were grown with vanillate, as indicated, and observed by video microscopy for 30 min. Box plots show the median number of cell reversals in 30 min (n=80 cells). Boxes depict quartiles and whiskers the maximum and minimum number of reversals that were observed. **(F)** The proportion of phosphorylated FrzZ protein increases only slightly upon FrzZ overexpression. Cell extracts of strain DZ4850 grown on agar plates containing vanillate, as indicated, were separated by SDS-PAGE containing 50 µM Phos-tag and analyzed by Western blot using FrzZ-specific anti-serum.

Figure 3: FrzE overexpression reduces cell reversals and FrzZ phosphorylation. **(A)** For controlled over-expression, a copy of FrzE was introduced in a *ΔfrzE* background under the control of an IPTG-inducible promoter (strain DZ4851, Δ*frzE* P_{IPTG}-*frzE*). **(B)** IPTG-dependent increase of FrzE concentration. Cell extracts of cells grown on CYE agar plates containing 0, 10 and 50 µM IPTG, respectively, were analyzed by Western blot using anti-FrzE specific antiserum. **(C)** Signal intensity for FrzE protein was quantified and normalized to wild type (mean±SD). Data represent three independent experiments. **(D)** FrzE overexpression affects cell motility and fruiting body formation. Strain DZ4851 was grown to exponential phase and was spotted to agar plates containing IPTG as indicated. **(E)** FrzE overexpression reduces the number of cell reversals. The number of cell reversals within 30 min were counted in individual cells grown at different IPTG concentrations. Box plots show the median number of cell reversals (n=80 cells), boxes enclose upper and lower quartiles, and whiskers extend to the maximum and minimum number of reversals that were observed. **(F)** FrzE overexpression abolishes phosphorylation of FrzZ. Cell extracts of strain DZ4851 grown on agar plates containing IPTG as indicated were separated by SDS-PAGE containing 50 µM Phos-tag, and analyzed by Western blot using FrzZ-specific anti-serum.

Figure 4: FrzZ overexpression alleviates the inhibitory effect of FrzE overexpression. **(A)** Strain DZ4852 (Δ*frzZ* Δ*frzE* P_{Van}-*frzZ* P_{IPTG}-*frzE*) containing independently inducible copies of FrzZ and FrzE was grown on agar plates containing different amounts of inducer, as indicated. **(B)** Cell reversals of individual cells of strain DZ4852 counted over a period of 30 min at different inducer concentrations. Box plots show the median number of cell reversals (n=80 cells), boxes enclose upper and lower quartiles, and whiskers extend to the maximum and minimum number of reversals that were observed. The dashed line indicates the mean number of cell reversals per 30 min detected in wild type. **(C)** FrzZ phosphorylation is restored upon simultaneous overexpression of FrzZ and

FrzE. Cell extracts of strain DZ4852 grown on agar plates containing different amounts of inducers, as indicated, were separated by SDS-PAGE containing 50 µM Phos-tag, and analyzed by Western blot using FrzZ-specific anti-serum and fluorescent secondary antibody.

Figure 5: The C-terminal domain of FrzE plays an important role in regulating cell reversals. **(A)** Strain DZ4853 (Δ*frzE* P_{IPTG}-*frzE*Δ^{cheY}) that expresses FrzEΔ^{CheY} from an IPTG-inducible promoter shows aberrant motility on 0.5% agar and is compromised in fruiting body formation at different amounts of inducer. **(B)** Cell reversal frequency does not change upon increasing IPTG concentration. The dashed line indicates the mean number of cell reversals per 30 min detected in wild type. **(C)** Cell extracts of strain DZ4853, grown with different amounts of inducer as indicated, were separated by SDS-PAGE containing 50 µM Phos-tag, and analyzed by Western blot using FrzZ-specific anti-serum. **(D)** Strain DZ4854 (Δ*frzE* P_{IPTG}-*frzE*^{D709A}) that expresses FrzE$^{\text{D709A}}$ from an IPTG-inducible promoter shows reduced motility on 0.5% agar and is compromised in fruiting body formation at different amounts of inducer. **(E)** Cell reversals are reduced, but not abolished, upon overexpression of FrzE$^{\text{D709A}}$. The dashed line indicates the mean number of cell reversals detected in wild type. **(F)** Strain DZ4854 shows a higher level of FrzZ phosphorylation, and phosphorylation does not change upon FrzE$^{\text{D709A}}$ overexpression. See legend to Figure 2 for experimental details.

Figure 6: Deletion of FrzZ can be compensated by expression of FrzE$^{\text{D709A}}$. FrzE under control of an IPTG-inducible promoter was introduced to a Δ*frzZ* Δ*frzE* double mutant to combine a Δ*frzZ* deletion with different FrzE variants. **(A)** Deletion of FrzZ in cells expressing the C-terminally truncated variant FrzEΔ^{CheY} results in hypo-reversing motility phenotypes on 0.5% agar and frizzy filaments on starvation agar. Strain DZ4869, which combines deletion of FrzZ with the expression of a point mutated variant of FrzE (FrzE$^{\text{D709A}}$) displays wild type-like behavior on soft agar and normal

fruiting body formation upon starvation. **(B)** Cell reversals on CYE agar counted over a period of 30 min in strains DZ4868 and DZ4869. A dashed line indicates the mean number of cell reversals per 30 min detected in wild type. Box plots show the median number of cell reversals (n=80 cells), boxes enclose upper and lower quartiles, and whiskers extend to the maximum and minimum number of reversals that were observed.

[a]Abbreviated description. The genotype of DZ4868 is *ΔfrzZ ΔfrzE* P_{IPTG}*-frzEΔ*^{cheY} and of DZ4869 *ΔfrzZ ΔfrzE* P_{IPTG}*-frzE*^{D709A}.

Figure 7: FrzE forms irregular clusters in the cell. (A) Motility phenotypes on 0.5% agar and starvation agar show that FrzE-YFP complements the function of the native protein. **(B)** Localization of FrzE-YFP. FrzE was fused to YFP and introduced into a *ΔfrzE* mutant background under the control of a vanillate inducible promoter (strain DZ4855, *ΔfrzE* P_{Van}*-frzE-yfp*). Fluorescence imaging of live cells was performed at basal expression levels without addition of inducer. Scale bar represents 5 μm.

Figure 8: FrzE co-localizes with FrzCD and with the nucleoid. (A) Simultaneous observation of FrzE-YFP, FrzCD-mCherry and DNA stained with Hoechst 33342. The localization of cellular clusters formed by FrzE-YFP (green) or FrzCD-mCherry (red) overlaps with the nucleoid (blue) in strain DZ4858 (*frzCD-mCherry* P_{Van}*-frzE-yfp*). **(B)** Signal intensity profiles corresponding to FrzE-YFP (green), FrzCD-mCherry (red) or Hoechst signals (blue). Pixel intensity is plotted against the position on the white line depicted in the bright field image in Fig. 8A. **(C)** FrzE-YFP localization depends on FrzCD and FrzA, but not on FrzZ. The FrzE-YFP fusion under control of a vanillate promoter was introduced into a *ΔfrzCD*, *ΔfrzA* or *ΔfrzZ* mutant background, respectively. Green: YFP signal, blue: Hoechst signal. **(D)** Signal intensity profiles corresponding to FrzE-YFP (green) or Hoechst signals (blue). Pixel intensity is plotted against the position on the white line depicted in the

bright field image in Fig. 8C. The different mutant backgrounds are indicated. Scale bars represent 5 μm.

Figure 9: FrzZ-GFP changes its localization upon deletion of FrzE-CheY. **(A)** FrzZ-GFP is dispersed in the cytoplasm and accumulates in a cluster at the leading cell pole. **(B)** The localization of FrzZ-GFP foci at the cell poles (green triangles) and full-length FrzE-mCherry clusters (red triangles) does not overlap in strain DZ4865 (*frzZ-gfp ΔfrzE* P_{Van}*-frzE-mCherry*). **(C)** FrzZ-GFP forms cellular clusters in addition to a polar focus when the C-terminal CheY-domain of FrzE is removed in strain DZ4857 (*frzE*Δ^{cheY} *frzZ-gfp*). **(D)** FrzZ-GFP and FrzEΔ^{CheY}-mCherry co-localize in cellular clusters (yellow triangles), but not at the cell pole. A vanillate-inducible copy of FrzE-mCherry or FrzEΔ^{CheY}-mCherry was introduced into a strain that expresses FrzZ-GFP under control of its native promoter (strain DZ4866, *frzZ-gfp ΔfrzE* P_{Van}*-frzE*Δ^{cheY}*-mCherry*). **(E)** FrzZ-GFP localizes at the cell pole when cells express FrzE$^{\mathrm{D709A}}$ (strain DZ4864, *frzZ-gfp ΔfrzE* P_{IPTG}*-frzE*^{D709A}). **(F)** FrzE$^{\mathrm{D709A}}$-YFP forms celluar clusters similar to FrzE-YFP (strain DZ4870, Δ*frzE* P_{Van}*-frzE*^{D709A}*-yfp*). Imaging was performed without addition of vanillate or IPTG, respectively. Scale bars represent 5 μm.

Figure 10: Three CheY-like domains modulate Frz signaling to regulate cell reversal frequency in *M. xanthus*. **(A)** The His-kinase FrzE is coupled via the FrzA protein to the receptor FrzCD, and to the nucleoid. Autophosphorylation of the CheA-like domain of FrzE is induced by FrzCD in response to an unknown stimulus. The phosphoryl-group is transferred from a histidine in FrzE to aspartate residues in its own C-terminal CheY-like domain, or to the CheY-like domains of the dual response regulator FrzZ. Phosphorylation of FrzZ and FrzE$^{\mathrm{CheY}}$ has activating and inhibiting effect on reversal frequency, respectively, but is not essential for signal transmission. FrzE directly or indirectly acts on downstream regulators at the cell poles to induce the polarity switch, which is

followed by re-orientation of the motility motors and cell reversal. **(B)** $FrzE^{CheY}$ and FrzZ accept phosphoryl-groups from the N-terminal CheA-like domain of FrzE, and phosphorylation of $FrzE^{CheY}$ inhibits FrzE autophosphorylation. Presumably, FrzZ acts as a positive regulator of FrzE activity by counteracting the negative effect of $FrzE^{CheY}$.

References

Amin, M., V.B. Kothamachu, E. Feliu, B.E. Scharf, S.L. Porter & O.S. Soyer, (2014) Phosphate sink containing two-component signaling systems as tunable threshold devices. *PLoS Comput Biol* **10**: e1003890.

Astling, D.P., J.Y. Lee & D.R. Zusman, (2006) Differential effects of chemoreceptor methylation-domain mutations on swarming and development in the social bacterium *Myxococcus xanthus*. *Mol Microbiol* **59**: 45-55.

Blackhart, B.D. & D.R. Zusman, (1985) "Frizzy" genes of *Myxococcus xanthus* are involved in control of frequency of reversal of gliding motility. *Proc Natl Acad Sci U S A* **82**: 8767-8770.

Bulyha, I., C. Schmidt, P. Lenz, V. Jakovljevic, A. Höne, B. Maier, M. Hoppert & L. Søgaard-Andersen, (2009) Regulation of the type IV pili molecular machine by dynamic localization of two motor proteins. *Mol Microbiol* **74**: 691-706.

Bustamante, V.H., I. Martínez-Flores, H.C. Vlamakis & D.R. Zusman, (2004) Analysis of the Frz signal transduction system of *Myxococcus xanthus* shows the importance of the conserved C-terminal region of the cytoplasmic chemoreceptor FrzCD in sensing signals. *Mol Microbiol* **53**: 1501-1513.

Campos, J.M., J. Geisselsoder & D.R. Zusman, (1978) Isolation of bacteriophage MX4, a generalized transducing phage for *Myxococcus xanthus*. *J Mol Biol* **119**: 167-178.

Guzzo, M., R. Agrebi, L. Espinosa, G. Baronian, V. Molle, E.M. Mauriello, C. Brochier-Armanet & T. Mignot, (2015) Evolution and Design Governing Signal Precision and Amplification in a Bacterial Chemosensory Pathway. *PLoS Genet* **11**: e1005460.

Hagen, D.C., A.P. Bretscher & D. Kaiser, (1978) Synergism between morphogenetic mutants of *Myxococcus xanthus*. *Dev Biol* **64**: 284-296.

Hodgkin, J. & D. Kaiser, (1979) Genetics of gliding motility in *Myxococcus xanthus* (Myxobacterales): Two gene systems control movement. *Mol Gen Genet* **171**: 177-191.

Inclán, Y.F., S. Laurent & D.R. Zusman, (2008) The receiver domain of FrzE, a CheA-CheY fusion protein, regulates the CheA histidine kinase activity and downstream signalling to the A- and S-motility systems of *Myxococcus xanthus*. *Mol Microbiol* **68**: 1328-1339.

Inclán, Y.F., H.C. Vlamakis & D.R. Zusman, (2007) FrzZ, a dual CheY-like response regulator, functions as an output for the Frz chemosensory pathway of *Myxococcus xanthus*. *Mol Microbiol* **65**: 90-102.

Iniesta, A.A., F. García-Heras, J. Abellón-Ruiz, A. Gallego-García & M. Elías-Arnanz, (2012) Two systems for conditional gene expression in *Myxococcus xanthus* inducible by isopropyl-β-D-thiogalactopyranoside or vanillate. *J Bacteriol* **194**: 5875-5885.

Jones, C.W. & J.P. Armitage, (2015) Positioning of bacterial chemoreceptors. *Trends Microbiol* **23**: 247-256.

Kaimer, C., J.E. Berleman & D.R. Zusman, (2012) Chemosensory signaling controls motility and subcellular polarity in *Myxococcus xanthus*. *Curr Opin Microbiol* **15**: 751-757.

Kaimer, C. & D.R. Zusman, (2013) Phosphorylation-dependent localization of the response regulator FrzZ signals cell reversals in *Myxococcus xanthus*. *Mol Microbiol* **88**: 740-753.

Keilberg, D., K. Wuichet, F. Drescher & L. Søgaard-Andersen, (2012) A response regulator interfaces between the Frz chemosensory system and the MglA/MglB GTPase/GAP module to regulate polarity in *Myxococcus xanthus*. *PLoS Genet* **8**: e1002951.

Kinoshita, E., E. Kinoshita-Kikuta & T. Koike, (2009) Separation and detection of large phosphoproteins using Phos-tag SDS-PAGE. *Nat Protoc* **4**: 1513-1521.

Leonardy, S., M. Miertzschke, I. Bulyha, E. Sperling, A. Wittinghofer & L. Søgaard-Andersen, (2010) Regulation of dynamic polarity switching in bacteria by a Ras-like G-protein and its cognate GAP. *EMBO J* **29**: 2276-2289.

Li, Y., V.H. Bustamante, R. Lux, D. Zusman & W. Shi, (2005) Divergent regulatory pathways control A and S motility in *Myxococcus xanthus* through FrzE, a CheA-CheY fusion protein. *J Bacteriol* **187**: 1716-1723.

Li, Y., H. Sun, X. Ma, A. Lu, R. Lux, D. Zusman & W. Shi, (2003) Extracellular polysaccharides mediate pilus retraction during social motility of *Myxococcus xanthus*. *Proc Natl Acad Sci U S A* **100**: 5443-5448.

Mauriello, E.M., (2013) Cell biology of bacterial sensory modules. *Front Biosci (Landmark Ed)* **18**: 928-943.

Mauriello, E.M., D.P. Astling, O. Sliusarenko & D.R. Zusman, (2009) Localization of a bacterial cytoplasmic receptor is dynamic and changes with cell-cell contacts. *Proc Natl Acad Sci U S A* **106**: 4852-4857.

Nan, B., M.J. McBride, J. Chen, D.R. Zusman & G. Oster, (2014) Bacteria that glide with helical tracks. *Curr Biol* **24**: R169-173.

Nan, B. & D.R. Zusman, (2011) Uncovering the mystery of gliding motility in the myxobacteria. *Annu Rev Genet* **45**: 21-39.

Paul, R., T. Jaeger, S. Abel, I. Wiederkehr, M. Folcher, E.G. Biondi, M.T. Laub & U. Jenal, (2008) Allosteric regulation of histidine kinases by their cognate response regulator determines cell fate. *Cell* **133**: 452-461.

Reichenbach, H., (1966) *Myxococcus spp*. (Myxobacterales): Schwarmentwicklung und Bildung von Protocysten. In: Publikationen zu wissenschaftlichen Filmen. Göttingen, Germany, pp. 557-578.

Reichenbach, H., (1993) Biology of myxobacteria: ecology and taxonomy. In: Myxobacteria II. M. Dworkin & D. Kaiser (eds). Washingston DC: Am. Soc. Microbiol., pp. 13-62.

Scott, A.E., E. Simon, S.K. Park, P. Andrews & D.R. Zusman, (2008) Site-specific receptor methylation of FrzCD in *Myxococcus xanthus* is controlled by a tetra-trico peptide repeat (TPR) containing regulatory domain of the FrzF methyltransferase. *Mol Microbiol* **69**: 724-735.

Shi, W. & D.R. Zusman, (1993) The two motility systems of *Myxococcus xanthus* show different selective advantages on various surfaces. *Proc Natl Acad Sci U S A* **90**: 3378-3382.

Sourjik, V. & R. Schmitt, (1998) Phosphotransfer between CheA, CheY1, and CheY2 in the chemotaxis signal transduction chain of Rhizobium meliloti. *Biochemistry* **37**: 2327-2335.

Spormann, A.M. & A.D. Kaiser, (1995) Gliding movements in *Myxococcus xanthus*. *J Bacteriol* **177**: 5846-5852.

Zhang, Y., M. Franco, A. Ducret & T. Mignot, (2010) A bacterial Ras-like small GTP-binding protein and its cognate GAP establish a dynamic spatial polarity axis to control directed motility. *PLoS Biol* **8**: e1000430.

Zhang, Y., M. Guzzo, A. Ducret, Y.Z. Li & T. Mignot, (2012) A dynamic response regulator protein modulates G-protein-dependent polarity in the bacterium *Myxococcus xanthus*. *PLoS Genet* **8**: e1002872.

Zusman, D.R., A.E. Scott, Z. Yang & J.R. Kirby, (2007) Chemosensory pathways, motility and development in *Myxococcus xanthus*. *Nat Rev Microbiol* **5**: 862-872.

Table 1: *M. xanthus* strains used in this study

	Relevant characteristics	Reference
DZ2	*wild type*	Campos *et al.* (1978)
DZ4481	*ΔfrzE*	Bustamante *et al.* (2004)
DZ4484	*ΔfrzZ*	Bustamante *et al.* (2004)
DZ4480	*ΔfrzCD*	Bustamante *et al.* (2004)
DZ4478	*ΔfrzA*	Bustamante *et al.* (2004)
DZ4849	*ΔfrzZ ΔfrzE*	this study
DZ4850	*ΔfrzZ* P_{Van}*-frzZ* kan^R	this study
DZ4851	*ΔfrzE* P_{IPTG}*-frzE* tet^R	this study
DZ4852	*ΔfrzZ ΔfrzE* P_{Van}*-frzZ* P_{IPTG}*-frzE* kan^R tet^R	this study
DZ4853	*ΔfrzE* P_{IPTG}*-frzE*Δ^{cheY} tet^R	this study
DZ4854	*ΔfrzE* P_{IPTG}*-frzE*^{D709A} tet^R	this study
DZ4868	*ΔfrzZ ΔfrzE* P_{IPTG}*-frzE*Δ^{cheY} tet^R	this study
DZ4869	*ΔfrzZ ΔfrzE* P_{IPTG}*-frzE*^{D709A} tet^R	this study
DZ4855	*ΔfrzE* P_{Van}*-frzE-yfp* kan^R	this study
DZ4856	*ΔfrzE* P_{Van}*-frzEΔcheY -yfp* kan^R	this study
DZ4857	*ΔfrzE* P_{Van}*-frzE*^{D709A}*-yfp* kan^R	this study
DZ4820	*frzCD-mCherry*	Mauriello & Zusman, unpublished
DZ4858	*frzCD-mCherry* P_{Van}*-frzE-yfp* kan^R	this study
DZ4859	*ΔfrzCD* P_{Van}*-frzE-yfp* kan^R	this study
DZ5860	*ΔfrzA* P_{Van}*-frzE-yfp* kan^R	this study
DZ4861	*ΔfrzZ* P_{Van}*-frzE-yfp* kan^R	this study
DZ4833	*frzZ-gfp*	Kaimer & Zusman (2013)
DZ4857	*frzE*Δ^{cheY} *frzZ-gfp*	this study
DZ4865	*frzZ-gfp ΔfrzE* P_{Van}*-frzE-mCherry* kan^R tet^R	this study
DZ4866	*frzZ-gfp ΔfrzE* P_{Van}*-frzE*Δ^{cheY}*-mCherry* kan^R tet^R	this study
DZ4864	*frzZ-gfp ΔfrzE* P_{IPTG}*-frzE*$^{D\square\square\square\square}$ kan^R tet^R	this study
DZ4870	*ΔfrzE* P_{Van}*-frzE*^{D709A}*-yfp* kan^R	this study

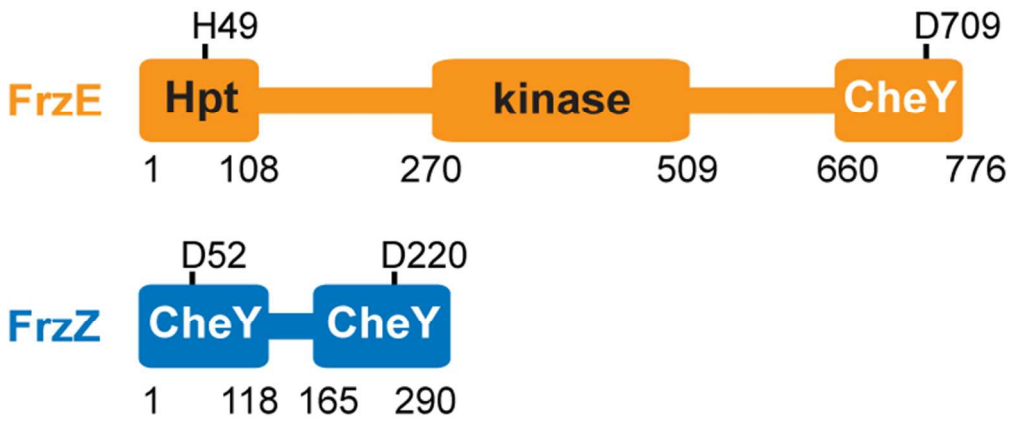

64x27mm (300 x 300 DPI)

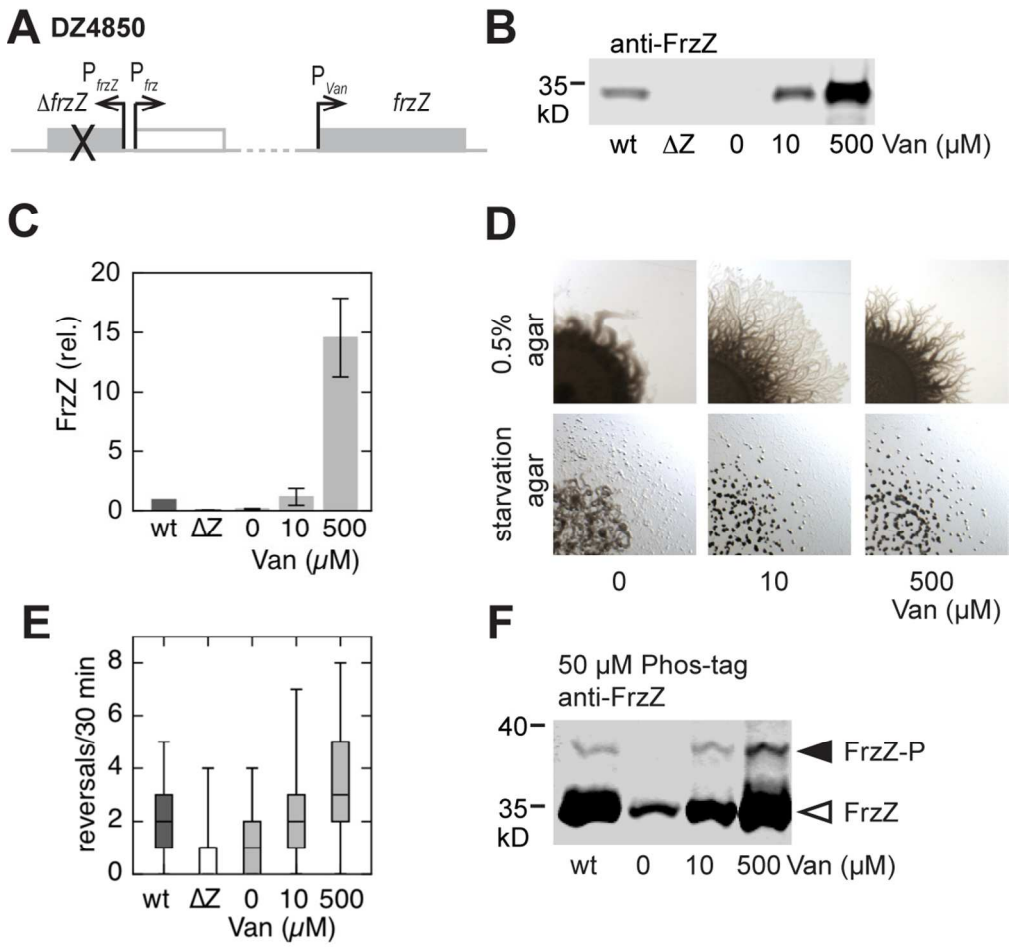

105x99mm (300 x 300 DPI)

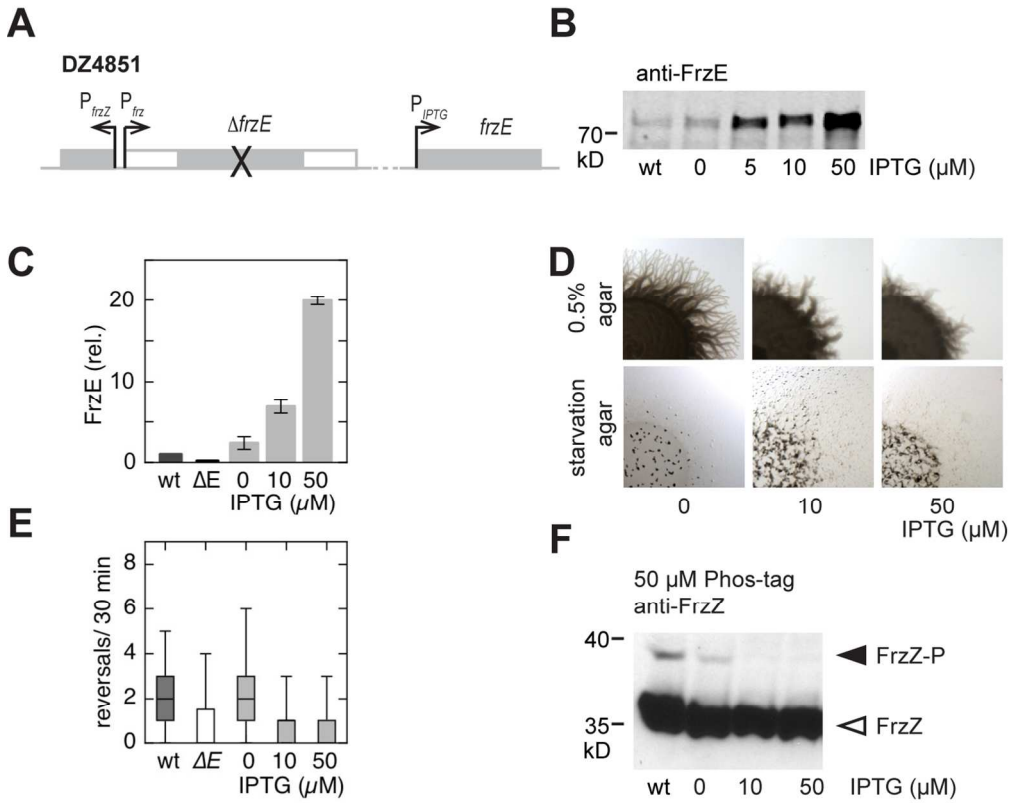

124x101mm (300 x 300 DPI)

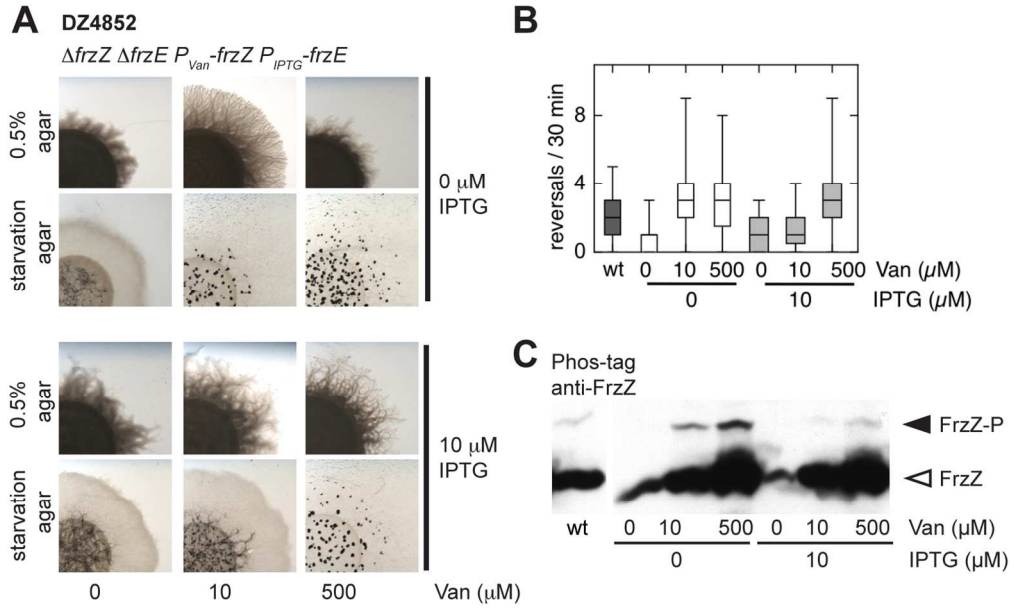

133x84mm (300 x 300 DPI)

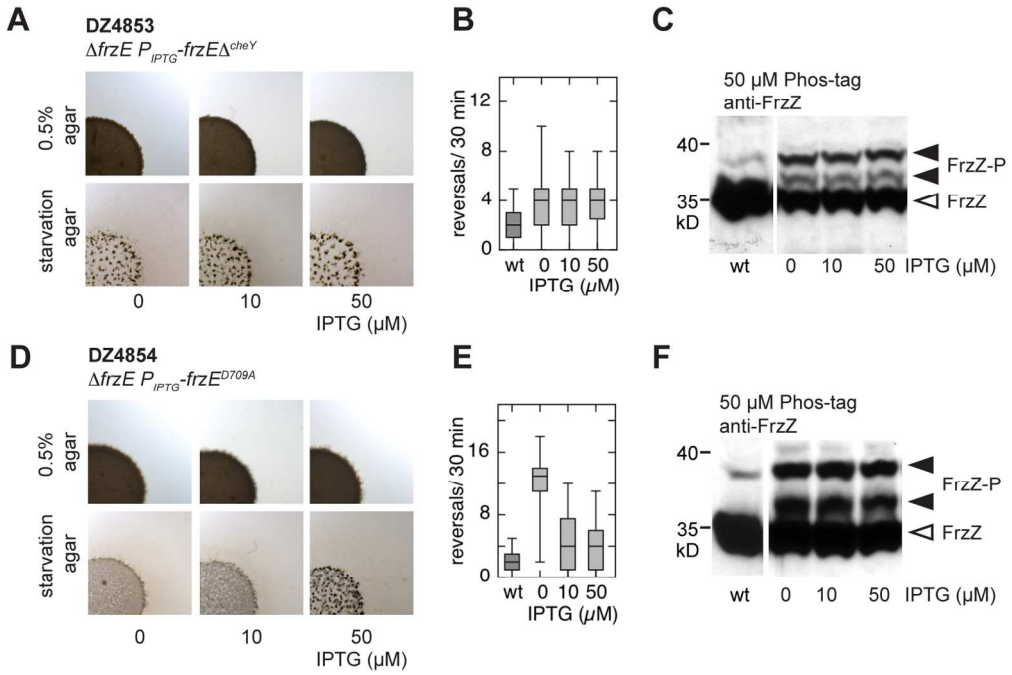

144x96mm (300 x 300 DPI)

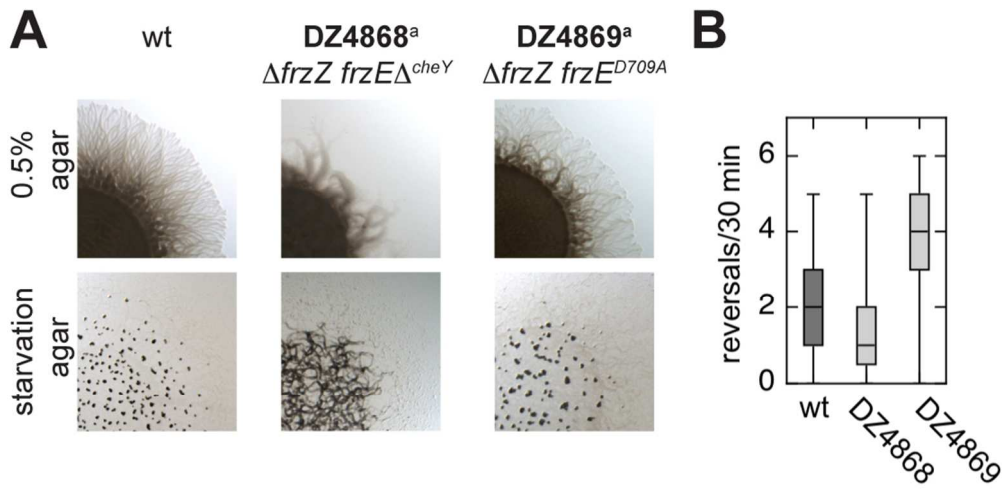

94x46mm (300 x 300 DPI)

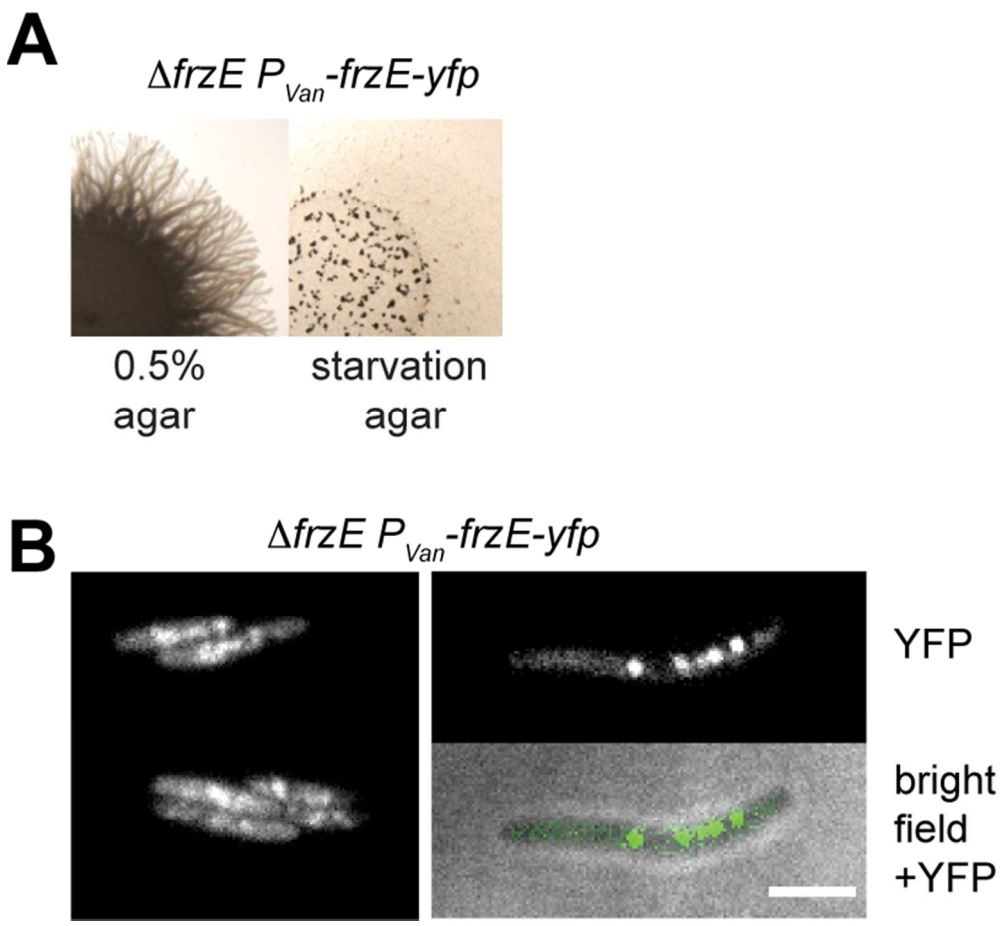

69x63mm (300 x 300 DPI)

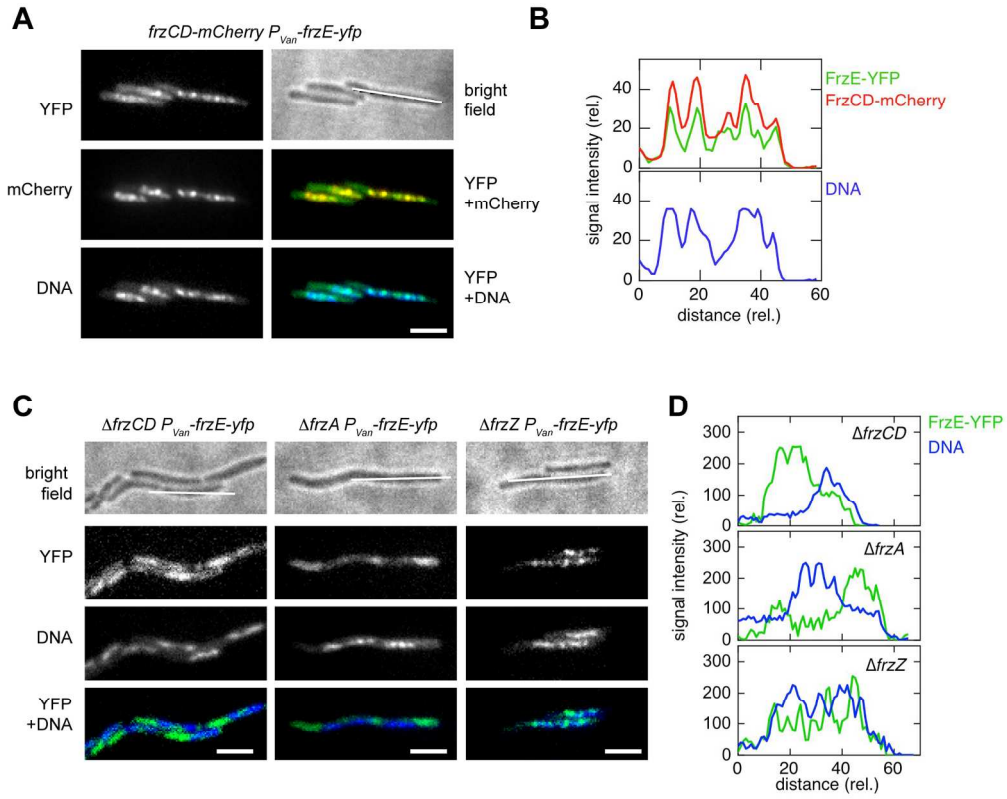

165x131mm (300 x 300 DPI)

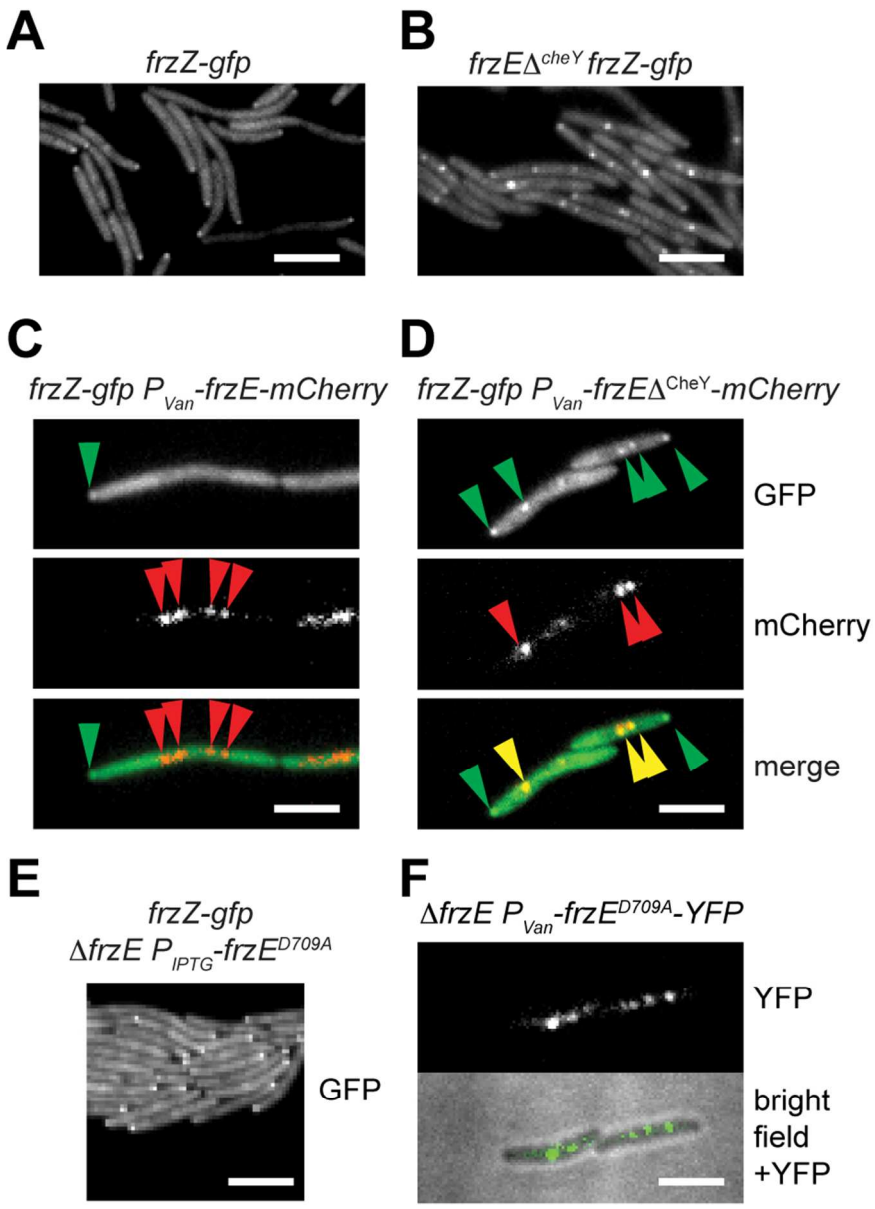

86x110mm (300 x 300 DPI)

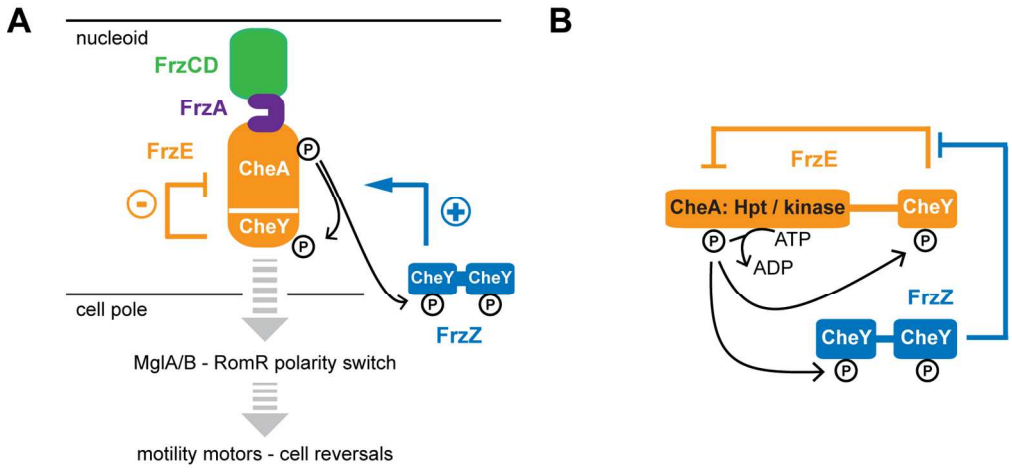

145x70mm (300 x 300 DPI)

The frequency of cell reversals in the gliding bacterium *Myxococcus xanthus* is controlled by the Frz two-component signaling pathway. Our experiments indicate that the response regulator domains of FrzZ positively modulate reversal frequency by counteracting the inhibitory activity of the CheY-like domain of FrzE. Thus the three CheY-like domains of the Frz pathway, $FrzE^{CheY}$ and $FrzZ^{CheY, CheY}$, constitute a regulatory unit to control the activity of the FrzE His-Kinase, a key component of the pathway.

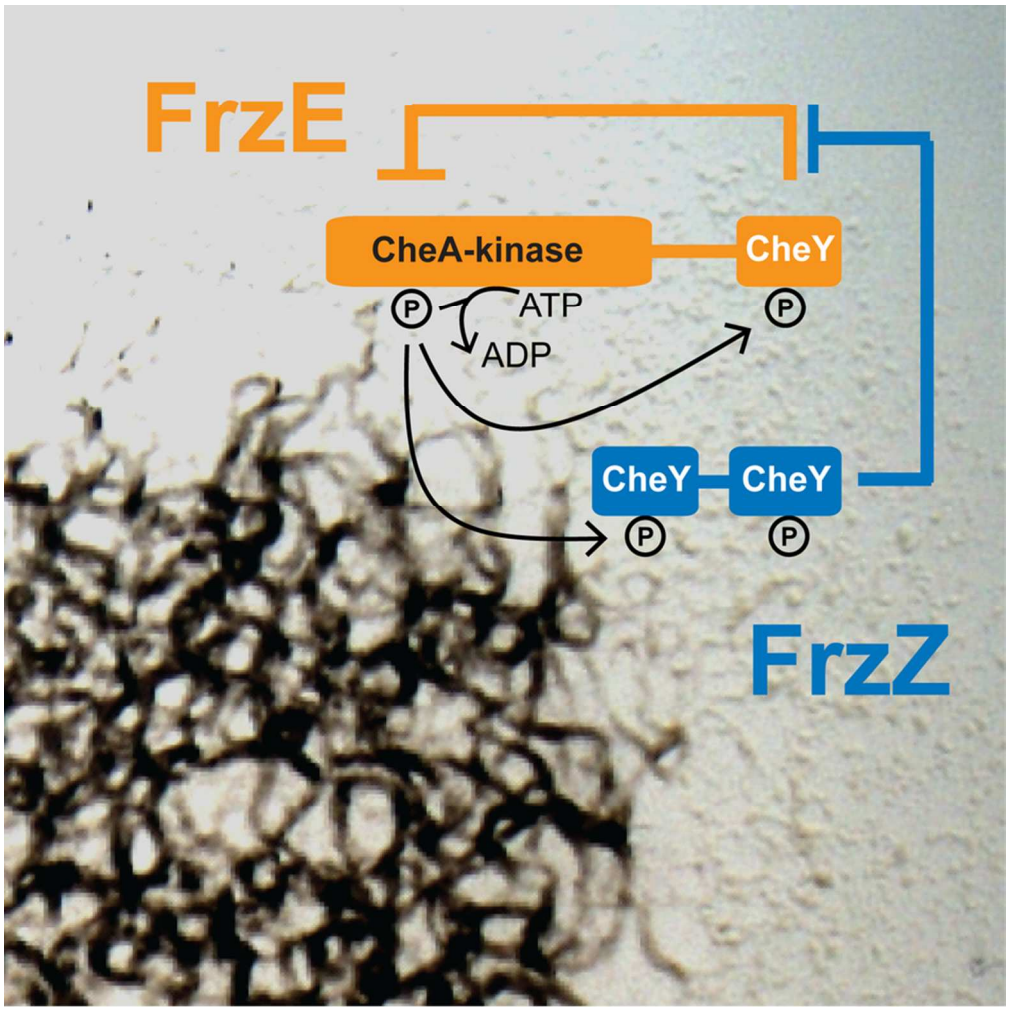

80x80mm (300 x 300 DPI)

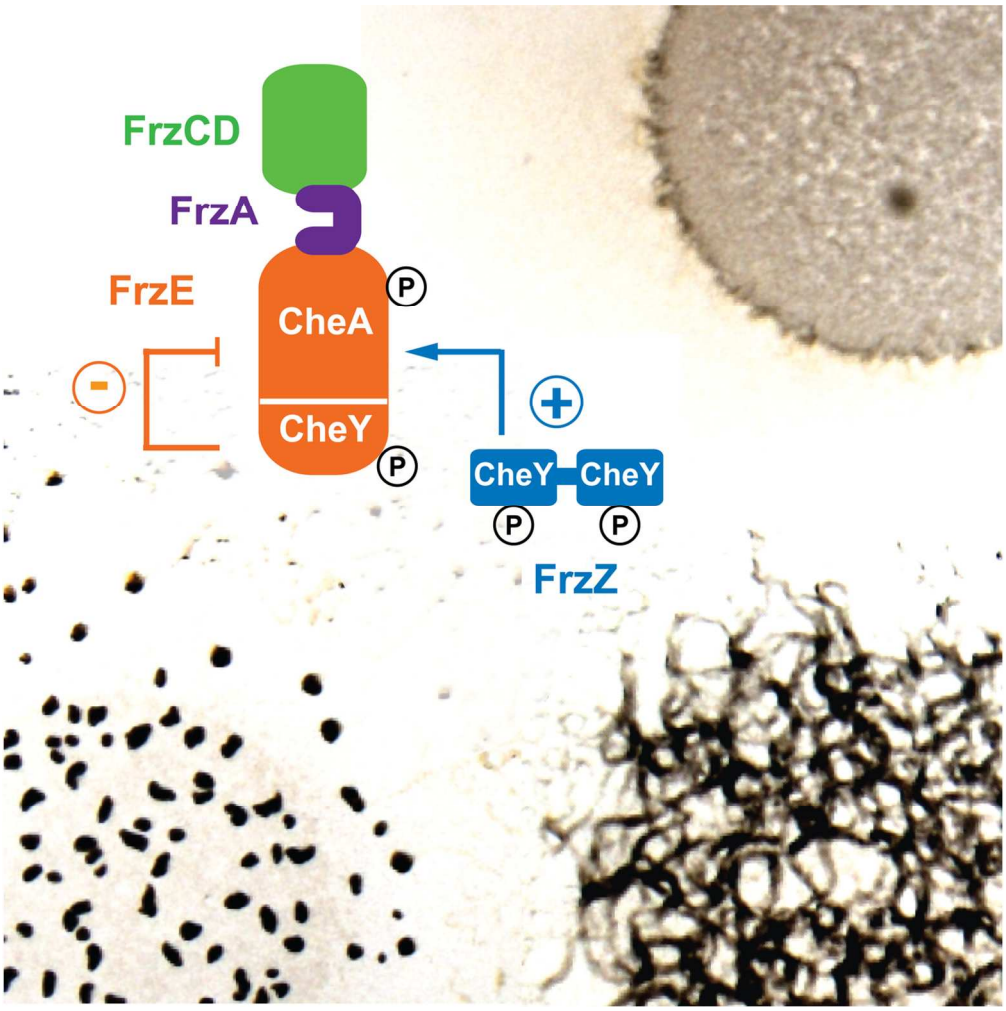

124x124mm (300 x 300 DPI)